Biosensors and Bioelectronics 213 (2022) 114437

Contents lists available at ScienceDirect

Biosensors and Bioelectronics

journal homepage: www.elsevier.com/locate/bios

A CRISPR-Cas12a-powered magnetic relaxation switching biosensor for the sensitive detection of *Salmonella*

Yafang Shen [a], Fei Jia [a,*], Yawen He [a], Yingchun Fu [a], Weihuan Fang [b], Jianping Wang [a], Yanbin Li [c,**]

[a] College of Biosystems Engineering and Food Science, Zhejiang University, Hangzhou, 310058, China
[b] College of Animal Sciences, Zhejiang University, Hangzhou, 310058, China
[c] Department of Biological and Agricultural Engineering, Center of Excellence for Poultry Science, University of Arkansas, Fayetteville, AR, 72701, USA

ARTICLE INFO

Keywords:
Magnetic relaxation switching
Magnetic nanoparticles
CRISPR-Cas12a
Salmonella detection

ABSTRACT

Magnetic relaxation switching (MRS) biosensors are attractive in the field of food safety owing to their simplicity and high signal-to-noise ratio. But they are less in sensitivity and stability caused by the insufficient crosslinking or non-specific binding of magnetic nanoparticles (MNPs) with targets. To address this problem, the CRISPR-Cas12a system was introduced into an MRS biosensor for the first time, to precisely control the binding of two types of MNPs with sizes of 130 nm (MNP_{130}) and 30 nm (MNP_{30}), for the sensitive detection of *Salmonella*. Delicately, the biosensor was designed based on the different magnetic properties of the two sizes of MNPs. The target *Salmonella* activated the collateral cleavage activity of the CRISPR-Cas12a system, which inhibited the binding of the two sizes of MNPs, resulting in an increase of unbound MNP_{30}. After separating MNP_{130}-MNP_{30} complexes and MNP_{130} from MNP_{30}, the free MNP_{30} left in solution acted as transverse relaxation time (T_2) signal reporters for *Salmonella* detection. Under optimized conditions, the CRISPR-MRS biosensor presented a limit of detection of 1.3×10^2 CFU mL^{-1} for *Salmonella*, which is lower than most MRS biosensor analogues. It also showed satisfactory specificity and performed well in spiked chicken meat samples. This biosensing strategy not only extends the reach of the CRISPR-Cas12a system in biosensors but also offers an alternative for pathogen detection with satisfactory sensitivity.

1. Introduction

Foodborne illnesses caused by pathogenic bacteria have become a big threat to human health and social economy (Kant et al., 2018; Xue et al., 2021). Among various pathogens, *Salmonella* receives one of the most concerns (Wang et al., 2019). It has been implicated in a considerable number of outbreaks of foodborne diseases and affects millions of people annually (Li et al., 2021; Srisa-Art et al., 2018). In the United States, *Salmonella* is estimated to cause approximately 1.35 million infections with 26,500 hospitalizations and 420 deaths every year (Centers for Disease Control and Prevention, 2022). *Salmonella* contaminations may find at each stage of the whole food supply chain and cause infection in human through the consumption of contaminated foods (Shen et al., 2021). The rapid and sensitive detection of *Salmonella* is the key to control the spread of *Salmonella* among foods and thus help prevent the outbreaks of *Salmonella*-related foodborne diseases.

Routine approaches for *Salmonella* detection mainly include culture plating, enzyme-linked immunosorbent assay (ELISA) and nucleic acid-based methods (Wang et al., 2020). However, some of them are sensitive and accurate but require several days for the verified results, and some are rapid and simple but may produce false positive or false negative results (Xu et al., 2022). Therefore, new methods are still needed for the sensitive, reliable and specific detection of *Salmonella* to ensure food safety.

In recent years, biosensors with different signal-transducing strategies have attracted increasing attention due to their advantages of high sensitivity, accuracy and specificity, low cost and simple operation (Fu et al., 2021; Hussain et al., 2022). Besides the commonly reported optical (Khansili et al., 2018), electrochemical (Gupta et al., 2021) and piezoelectric (Jandas et al., 2021) biosensors, magnetic relaxation switching (MRS) biosensors, which were based on the magnetic relaxation characteristics of magnetic nanoparticles (MNPs), have shown

* Corresponding author.
** Corresponding author.
E-mail addresses: fei_jia@zju.edu.cn (F. Jia), yanbinli@uark.edu (Y. Li).

https://doi.org/10.1016/j.bios.2022.114437
Received 18 March 2022; Received in revised form 10 May 2022; Accepted 27 May 2022
Available online 6 June 2022
0956-5663/© 2022 Elsevier B.V. All rights reserved.

great potential in the field of food safety due to their advantages of low background signal and high simplicity (Dong et al., 2021; Wang and Lin, 2020). The MRS nanobiosensor was first reported by Weissleder and co-workers (Josephson et al., 2001). Thereafter, many MRS biosensors were investigated for the detection of various target analytes (Dong et al., 2022; Huang et al., 2021; Kaittanis et al., 2007; Tsourkas et al., 2004). When the aggregation (or disaggregation) state of MNPs changes, the transverse relaxation time (T_2) of the surrounding water protons changes accordingly (Chen et al., 2015; Hong et al., 2021). Therefore, T_2 can work as a signal output for target analytes detection. However, the non-specific aggregation of MNPs owing to their high surface energy may influence the overall stability and accuracy (Wang and Lin, 2020; Xianyu et al., 2021). To address this problem, MRS biosensors based on the concentration change of MNPs have been developed (Chen et al., 2015; Jia et al., 2021; Qi et al., 2021). In such assays, however, the sensitivity may be compromised as a result of the insufficient cross-linking or non-specific binding of MNPs with targets. Therefore, new strategies to precisely control the binding of MNPs are necessary.

Clustered regularly interspaced short palindromic repeats (CRISPR), derived from gene-editing technology, is emerged as a useful tool in the field of biosensing (Bruch et al., 2019; Phan et al., 2022; Sheng et al., 2021; Yue et al., 2021). Notably, the CRISPR-Cas12a system, with a collateral cleavage behavior, receives particular attention due to its outstanding features in easy using, low-cost and high stability. Cas12a is a kind of RNA-guided endonuclease that not only serves as a target-specific cleavage effector but also presents *trans*-cleavage activity on random single-stranded DNAs (ssDNAs) (Dai et al., 2020; Kachwala et al., 2021). Upon recognition and cleavage of the target DNA with the assistance of a designed CRISPR RNA (crRNA), the collateral cleavage activity of Cas12a is activated, which can trigger the indiscriminate digestion of surrounding ssDNAs (Gong et al., 2021; Kachwala et al., 2021). This property makes CRISPR-Cas12a a new sensing tool through the cleavage of custom ssDNAs. By using ssDNA labeled with both fluorophore and quencher as the reporter probe, fluorescent approaches, as represented by the DETECTR platform, have been well developed (Chen et al., 2018). Thereafter, many other types of CRISPR-Cas12a-based biosensors with colorimetric (Cao et al., 2021), electronic (Nouri et al., 2021), surface-enhanced Raman scattering (Choi et al., 2021) and other forms of signal output also have been proposed, further showing the versatility of the CRISPR-Cas12a system. However, research on MRS biosensors with the assistance of the CRISPR-Cas12a system is still in its infancy.

Inspired by the merits of both MRS sensing and the CRISPR-Cas12a system, we herein report a CRISPR-MRS biosensor. Different from conventional MRS biosensors, we use two types of MNPs with different sizes for magnetic separation and signal output, respectively, and introduce the CRISPR-Cas12a system to precisely control the coupling of the two sizes of MNPs. The detection specificity can be improved markedly owing to the high recognition accuracy of the CRISPR-Cas12a system. And the inherent signal amplification of the CRISPR-Cas12a system (Wang et al., 2021) also contributes to an enhanced detection sensitivity. Two different cleavage strategies were systematically studied, offering the guidance for the development of CRISPR-Cas12a-based biosensors. Moreover, aided by the CRISPR-Cas12a system to precisely control the binding of the two sizes of MNPs, it avoided the non-specific binding or insufficient cross-linking of MNPs with targets in conventional MRS methods and therefore improve the stability and reliability of the biosensor. The proposed CRISPR-MRS biosensor is not only successfully applied to the sensitive and specific detection of *Salmonella*, but also has the potential to be extended to detect other pathogens, providing a reliable tool to enhance the safety of the food supply chain.

2. Experimental section

2.1. Bacterial culture, plating and DNA extraction

The stock culture of *Salmonella* Typhimurium from a −80 °C freezer was grown in brain heart infusion (BHI) broth at 37 °C for 18–20 h. Then, the culture containing *S*. Typhimurium was centrifugated at 6000 rpm for 5 min and washed with sterile phosphate buffered saline (PBS). The washed culture was serially diluted in PBS and incubated onto a xylose-lysine-tergitol 4 (XLT4) agar for 24 h to determine colony numbers. Finally, genomic DNA of *S*. Typhimurium was extracted via a boiling method and the DNA extracts were stored at −20 °C for further use. For safety considerations, all the above tests were conducted in a biosafety level 2 laboratory.

2.2. Polymerase chain reaction

Amplicons of *S*. Typhimurium genomic DNA were obtained via polymerase chain reaction (PCR). The reactions were carried out in a total volume of 30 μL containing 15 μL of PCR Master Mix, 11 μL of ddH_2O, 1 μL of forward primers (10 μM), 1 μL of reverse primers (10 μM) and 2 μL of template DNA. The sequence information of the primers is shown in Table S1. After an initial denaturation at 98 °C for 3 min, 32 cycles of amplification were performed (denaturation at 98 °C for 10 s, annealing at 57 °C for 5 s and extension at 68 °C for 5 s).

2.3. CRISPR-MRS sensing of Salmonella

MNPs with diameters of around 130 nm (MNP_{130}) and 30 nm (MNP_{30}) were modified with streptavidin (SA) and ssDNA (biotin-S_2) to prepare MNP_{130}-SA and MNP_{30}-S_2 probes, respectively. 20 μL of PCR amplicons were mixed with 200 nM Cas12a protein, 250 nM crRNA, 10 U RNase inhibitor, 1 × NEBuffer 2.1 and 200 nM biotin-S_1. Then the CRISPR-Cas12a-mediated cleavage assay was carried out at 37 °C for 20 min. Afterwards, 30 μL of MNP_{130}-SA probes together with 120 μL of 10 mM PBS with 0.01% Tween-20 (PBST) were added, and the mixture was incubated on a rotator for 10 min for the capture of biotin-S_1 fragments. After magnetic separation, the pellet was re-suspended in 190 μL of PBST, followed by the addition of 10 μL of MNP_{30}-S_2. After reaction for 45 min at ambient temperature, magnetic separation was performed by using a magnetic scaffold. Finally, 190 μL of the supernatant was collected, diluted with 810 μL of deionized water and placed in a low-field nuclear magnetic resonance (LF-NMR) instrument for T_2 measurement. The sequence information of biotin-S_1, biotin-S_2 and crRNA, the preparation of MNP_{130}-SA, MNP_{30}-S_2 and chicken meat samples, and data analysis are shown in supporting material.

3. Results and discussion

3.1. Detection principle of the CRISPR-MRS biosensor

The key principle of the CRISPR-MRS biosensor relies on the CRISPR-Cas12a system to precisely control the binding of MNP_{130} for magnetic separation and MNP_{30} for signal output (Scheme 1). First, SA and biotin-S_2 are modified on the surface of MNP_{130} and MNP_{30} to prepare MNP_{130}-SA and MNP_{30}-S_2 probes, respectively. The two probes can be linked by a complementary biotin modified ssDNA (biotin-S_1) as linkers. In the presence of *Salmonella*, the collateral cleavage activity of the CRISPR-Cas12a system is activated, resulting in the degradation of biotin-S_1. Therefore, the binding of MNP_{130}-SA and MNP_{30}-S_2 is inhibited, leaving abundant free MNP_{30}-S_2 probes in the solution. Due to their different saturation magnetizations, MNP_{130}-MNP_{30} complexes and MNP_{130}-SA can be separated very quickly in an applied magnetic field, while MNP_{30}-S_2 probes cannot be separated and show well-dispersed in the solution. After magnetic separation, the unbound MNP_{30}-S_2 left in the solution can serve as T_2 signal reporters. Under the condition that a

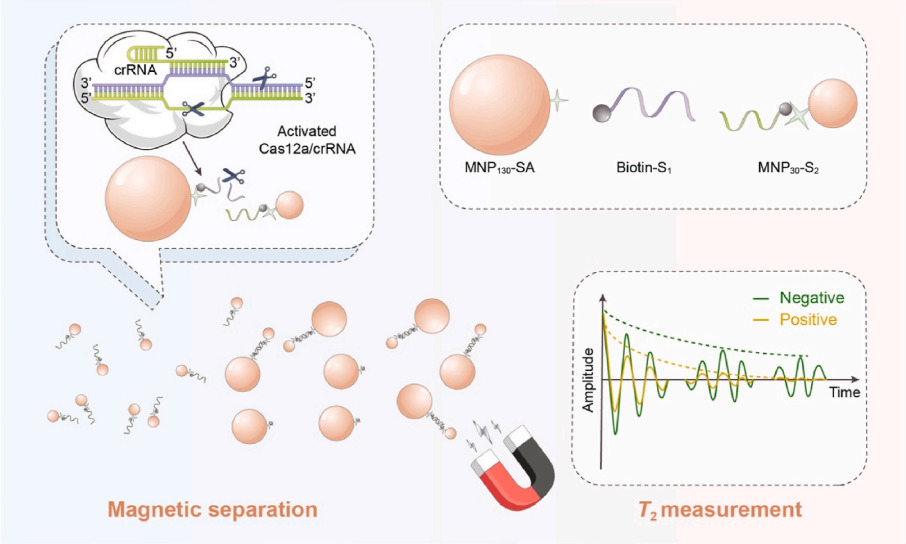

Scheme 1. Illustration of the CRISPR-MRS biosensor for *Salmonella* detection.

constant amount of MNP_{30}-S_2 probes is introduced, the amount of free MNP_{30}-S_2 after reaction is dependent upon the collateral cleavage activity of the CRISPR-Cas12a system and thus correlates to the concentration of target *Salmonella*. When there are no targets existing, only a small number of free MNP_{30}-S_2 probes are left because most of them bind to the surface of MNP_{130}-SA and are easily magnetically separated, resulting in a high T_2 value. On the other hand, the presence of targets activates the CRISPR-Cas12a system, which can hinder the binding of the MNP_{130}-SA and MNP_{30}-S_2 probes, leading to an increased amount of unbound MNP_{30}-S_2 and a low T_2 value.

3.2. Feasibility of the CRISPR-MRS biosensor for Salmonella detection

In this CRISPR-MRS biosensor, the different magnetic behaviors of MNP_{130} and MNP_{30} in the same magnetic field were exploited. First, the separation efficiency of the two sizes of MNPs was evaluated. As shown in Fig. 1A, MNP_{130} and MNP_{30} were placed in the same magnetic field. We saw that MNP_{130} was rapidly accumulated to the bottom of the vial due to its high saturation magnetization, whereas MNP_{30} with a low saturation magnetization was still well-dispersed in solution after 10 min, showing the significant difference on the magnetic separation speed between the two types of MNPs. The same results can be found in the time course T_2 measurement test as well. Both MNP_{130} and MNP_{30} were placed in a same magnetic scaffold and the T_2 values of the supernatant at different magnetic separation time points were measured. For MNP_{30}, there was merely an imperceptible change in the T_2 value at different time points. For MNP_{130}, however, the T_2 value increased sharply from 94 to 1455 ms during the first 10 min of separation and

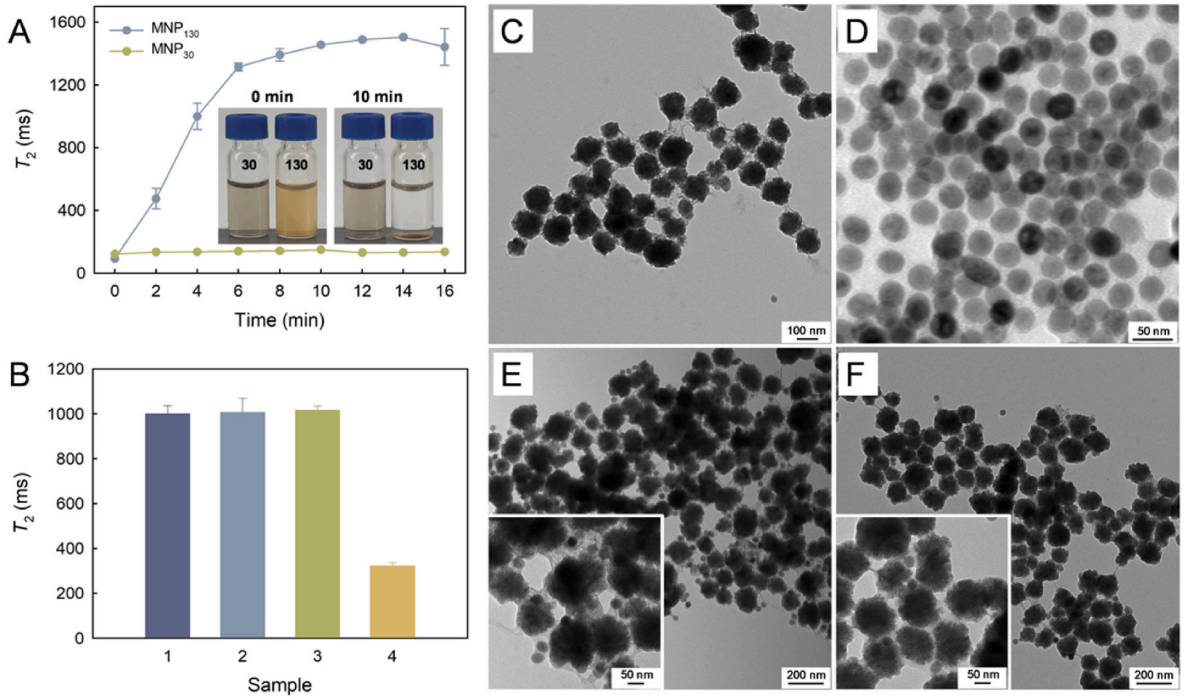

Fig. 1. (A) The magnetic separation efficiency of MNP_{130} and MNP_{30}. (B) The T_2 values of samples with (1) Cas12a, (2) Cas12a and crRNA, (3) Cas12a and target DNA and (4) Cas12a, crRNA and target DNA. TEM images of (C) MNP_{130}-SA, (D) MNP_{30}-S_2 and MNP_{130}-SA (E) in the absence and (F) in the presence of target DNA.

then leveled out as a result of the migration of MNP_{130} in the magnetic field. These results indicated that MNP_{130} could be effectively separated from MNP_{30} when a magnetic field applied.

Then, the recognition and collateral cleavage abilities of the CRISPR-Cas12a system were investigated. The *invA* gene, which is conserved among nearly all *Salmonella* spp.(Chun et al., 2018), was chosen as the target and the amplicons of the *invA* gene fragment were obtained via PCR amplification. Agarose gel electrophoresis confirms the successful amplification of the *invA* gene fragment (Fig. S1). Also, a crRNA targeting a 23-bp region of the *invA* gene was designed for specific recognition of *Salmonella*. When it recognized the target gene, the CRISPR-Cas12a system was activated and showed *trans*-cleavage activity to surrounding biotin-S_1, which in turn affected the binding of MNP_{130}-SA and MNP_{30}-S_2 probes and caused a decrease in the T_2 value. As shown in Fig. 1B, for samples that coexisted with target amplicons, Cas12a and crRNA, the T_2 value dropped dramatically with a decrease rate reaching over 60%. For reference, however, a barely notable change in T_2 value (<1.5%) was observed without crRNA or target DNA. These results indicated that the Cas12a/crRNA complexes could accurately recognize the *invA* gene of *Salmonella* and initiate its *trans*-cleavage activity to precisely control the binding of MNP_{130} and MNP_{30}.

Moreover, transmission electron microscope (TEM) was also used to characterize the morphologies of the two kinds of MNPs. As shown in Fig. 1C and D, the average particle sizes for MNP_{130}-SA and MNP_{30}-S_2 were approximately 130 nm and 30 nm, respectively. In the absence of target DNA, abundant MNP_{30} was clearly observed on the surface of MNP_{130} due to the binding of the two probes (Fig. 1E). In the presence of target DNA, however, the activated CRISPR-Cas12a system inhibited the linking of the two probes, resulting in a limited number of MNP_{30} binding on the MNP_{130} surface (Fig. 1F). Taken together, these results demonstrated the feasibility of the CRISPR-MRS biosensor for *Salmonella* detection.

3.3. Comparation of the two cleavage strategies

It is reported that the CRISPR-Cas12a system shows the *trans*-cleavage activity not only to ssDNAs in the solution but also to those on the nanoparticle surface (Fu et al., 2021). Therefore, both free biotin-S_1 and biotin-S_1 modified on the surface of MNP_{130} (MNP_{130}-S_1) can be used as the cleavage substrates (Fig. 2A). The analytical performances of the CRISPR-MRS biosensors based on the cleavage of MNP_{130}-S_1 and free biotin-S_1 were systematically studied. As shown in Fig. 2B, when MNP_{130}-S_1 was used for cleavage, an input amount of 10^5 CFU mL^{-1} of *Salmonella* only resulted in an approximately 25% decline in the T_2 value. Though the detection sensitivity was not satisfactory, however, an obvious difference in the dispersion state of MNP_{130} was observed. As shown in the inset of Fig. 2B, in the absence of the target, impressively, a large amount of MNP_{130} precipitated to the bottom of the tube due to the increased gravitational potential energy when binding with MNP_{30}, whereas the particles were still well dispersed in the presence of the *Salmonella* because the binding of the two types of MNPs was inhibited by the activated CRISPR-Cas12a system. When using free biotin-S_1 as the cleavage substrates, the detection sensitivity can be significantly improved. The T_2 value declined by approximately 60% in the presence of *Salmonella* (Fig. 2C). But MNP_{130} both in the negative and positive samples were almost equally well-dispersed when the reaction was finished (Fig. 2C inset). The aforementioned results are interesting and may be explained by the stability of the MNP_{130}. When MNP_{130}-S_1 was added into the CRISPR-Cas12a reaction buffer for cleavage, their colloidal stability may be severely reduced due to the complex buffer conditions, which makes them more susceptible to gravity effects. Thus, in the absence of the target, the unstable MNP_{130} reacted with MNP_{30} and then rapidly sedimented. However, the binding sites on MNP_{130} surface were also blocked along with the settling of the nanoparticles, making it much easier to be saturated. Therefore, as evidenced by the low T_2 value in the absence of the target in Fig. 2B, a considerable amount of MNP_{30}-S_2 probes were left in the solution. As a result, when MNP_{130}-S_1 was used for cleavage, the detection sensitivity was also decreased because of the reduced binding sites on the surface of the MNP_{130}, although a significant difference in the dispersion state of MNP_{130} was observed. For cleavage of free biotin-S_1, MNP_{130} kept stable and could provide abundant binding sites for MNP_{30}. Therefore, though no distinguishable difference in the dispersion state of MNP_{130} was observed, the detection sensitivity was significantly improved. Therefore, for qualitative or semi-quantitative discrimination, where sensitivity is not a primary concern, using MNP_{130}-S_1 for cleavage is proved to be a suitable choice; whereas for more sensitive detection of *Salmonella*, cleaving free biotin-S_1 would be more appropriate. In this study, free biotin-S_1 was chosen as the substrates in view of the detection sensitivity.

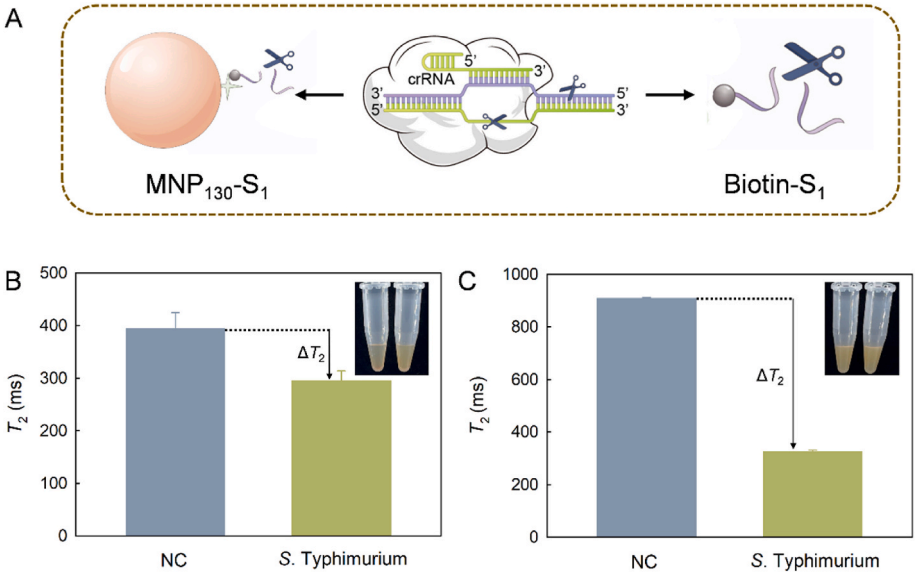

Fig. 2. (A) Illustration of the *trans*-cleavage of MNP_{130}-S_1 and free biotin-S_1. Comparation of the T_2 values with the cleavage of (B) MNP_{130}-S_1 and (C) free biotin-S_1, and (insets) the dispersion states of MNP_{130} in the absence (left) and in the presence (right) of the target.

3.4. Optimization of assay parameters

To improve the analytical performance of the CRISPR-MRS biosensor, several important assay parameters were optimized, including the concentration of biotin-S_1, the volume of MNP_{130}-SA, and the reaction time for Cas12a cleavage, MNP_{130}-SA capture of biotin-S_1 and MNP_{30}-S_2 binding to the surface of MNP_{130}-SA (Fig. 3A).

First, the effects of biotin-S_1 and MNP_{130}-SA concentrations on the MRS signal response were investigated. As *trans*-cleavage substrates, the concentration of biotin-S_1 is one of the most important parameters that may affect the sensitivity of the CRISPR-MRS biosensor. As shown in Fig. 3B, the T_2 value increased continuously with the increase of biotin-S_1 concentration because more MNP_{30}-S_2 could bind to the surface of MNP_{130}-SA with the assistance of the biotin-S_1. However, the detection sensitivity may be compromised with an excess amount of biotin-S_1 due to the possible insufficient *trans*-cleavage. $\Delta T_2\%$ ($\frac{Background\ signal - Target\ signal}{Background\ signal} \times 100\%$) reached a maximum when the biotin-S_1 concentration was 200 nM, indicating a satisfactory sensitivity could be obtained at that concentration. Hence, an optimized biotin-S_1 concentration of 200 nM was selected for Cas12a cleavage. Apart from biotin-S_1, the concentration of MNP_{130}-SA is also essential for the detection sensitivity. MNP_{130}-SA plays an important role in the capture of biotin-S_1 and further providing binding sites for MNP_{30}-S_2. To explore its effect on *Salmonella* detection, MNP_{130}-SA with different volumes of 10–50 μL were added to see the difference. Fig. 3C shows that the $\Delta T_2\%$ increased with the increasing amount of MNP_{130}-SA from 10 to 30 μL and reached a platform thereafter. Thus, 30 μL of MNP_{130}-SA was the optimized concentration and can be used in the following tests.

The reaction time for Cas12a cleavage, MNP_{130}-SA capture of biotin-S_1 and MNP_{30}-S_2 binding to the surface of MNP_{130}-SA was also evaluated. It is reported that the *cis*-cleavage of target DNAs by the CRISPR-Cas12a system is generally completed within 30 min, whereas the *trans*-cleavage of non-targeted ssDNAs can last for more than 3 h (Dai et al., 2019). In this study, the T_2 value dropped dramatically during the first 20 min and then continued to decrease but much slowed down (Fig. 3D), indicating that most of the biotin-S_1 can be non-specifically cleaved within 20 min. After a thorough consideration of the detection time and the sensitivity, the cleavage time was optimized to 20 min. Subsequently, the incubation time of MNP_{130}-SA for the capture of biotin-S_1 and the binding time between MNP_{130}-SA and MNP_{30}-S_2 were also investigated. The capture of biotin-S_1 could be finished within 10 min due to the fast binding kinetics between biotin and SA (Fig. 3E) (Srisa-Art et al., 2008). For MNP_{30}-S_2 binding, Fig. 3F indicates that the optimum time was 45 min and the change of the T_2 value was fairly small after 45 min binding time.

3.5. Analytical performance of the CRISPR-MRS biosensor for *Salmonella* detection

Under the optimized conditions, the analytical performance of the CRISPR-MRS biosensor for *Salmonella* detection was further evaluated. Genomic DNAs were extracted from *S.* Typhimurium cells and amplified by PCR. Then, the amplicons were used directly for detection (Fig. 4A). As shown in Fig. 4B, the T_2 value decreased accordingly with the increase of *S.* Typhimurium concentration and the measured data points was fitted to a four-parameter logistic curve. The linear detection range was from 10^2 to 10^6 CFU mL^{-1} (Fig. S2). Based on the 3σ standard rule, the CRISPR-MRS biosensor was capable of detecting *S.* Typhimurium at

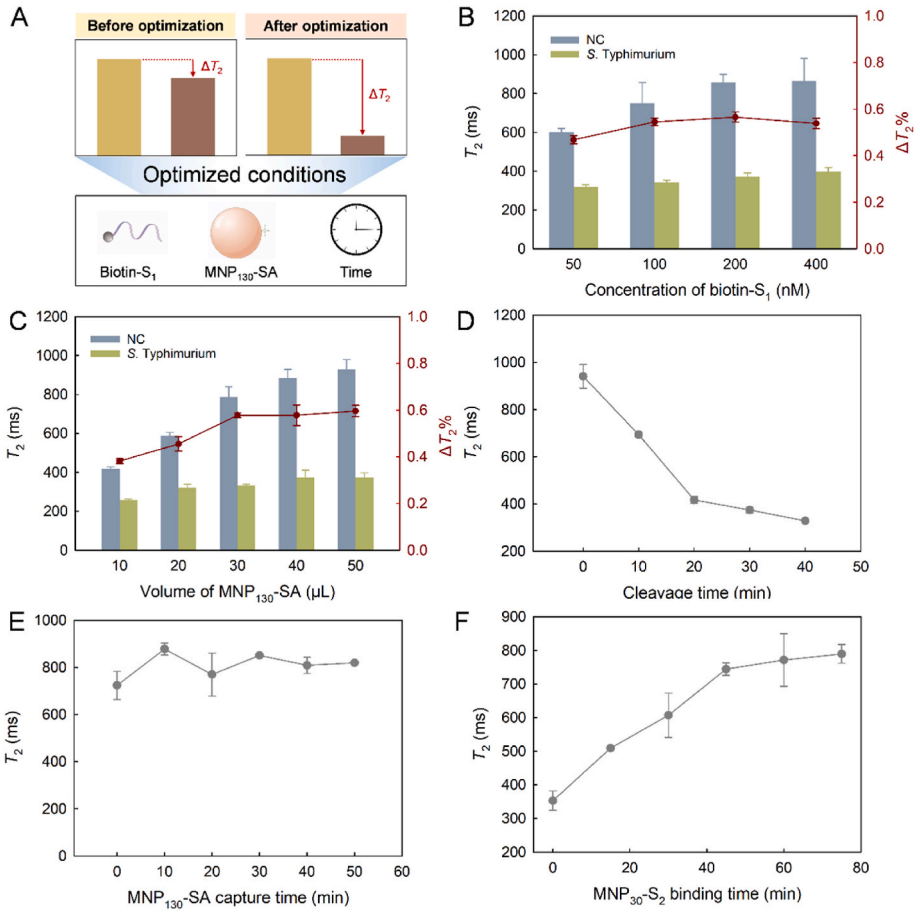

Fig. 3. (A) Illustration of optimized assay parameters. Optimization of (B) biotin-S_1 concentration, (C) the added volume of MNP_{130}-SA and reaction time for (D) Cas12a cleavage, (E) MNP_{130}-SA capture of biotin-S_1 and (F) MNP_{30}-S_2 binding to the surface of MNP_{130}-SA.

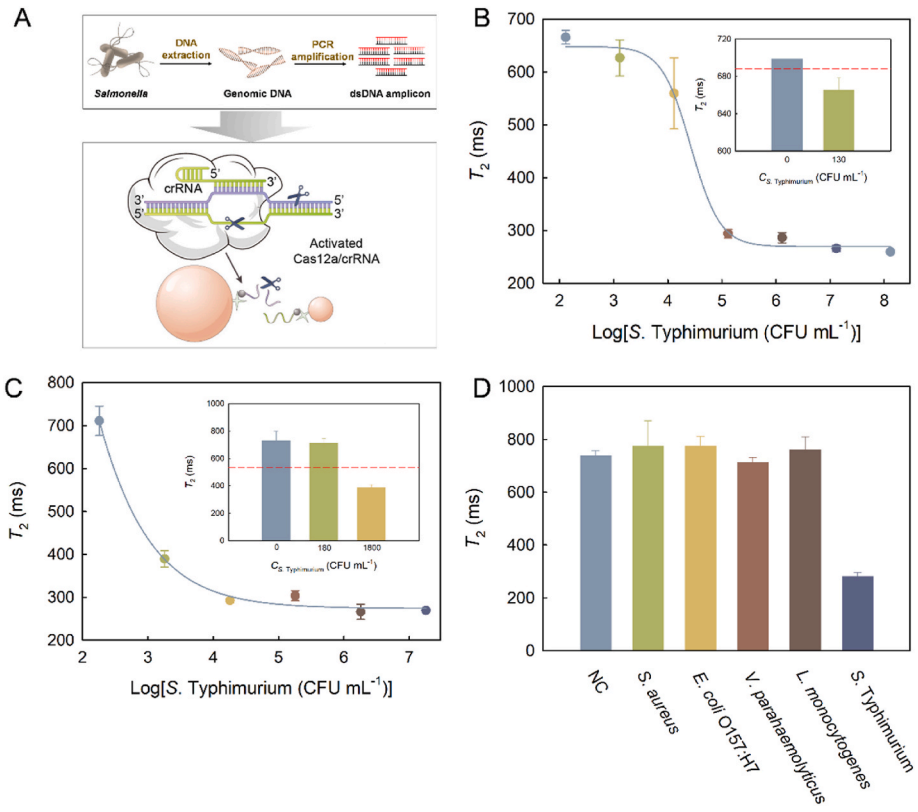

Fig. 4. (A) Illustration of the workflow of the CRISPR-MRS biosensor for *Salmonella* detection. Dynamic ranges for detection of *S*. Typhimurium in (B) pure culture and (C) chicken breast extracts. The threshold lines (red dotted) represent mean - three standard deviations (negative control). (D) Selectivity of the CRISPR-MRS biosensor.

levels as low as 1.3×10^2 CFU mL^{-1}, which was better than most of other MRS biosensors (Table S2). It should be noted that the T_2 value dropped dramatically when the concentration of *S*. Typhimurium reached 10^5 CFU mL^{-1} and then kept decreasing but with a much slower speed. This was caused by the high turnover rate of the Cas12a/crRNA complex (Bao et al., 2020). With high *S*. Typhimurium concentrations, the Cas12a/crRNA complex get fully activated. Therefore, it degrades most of the surrounding biotin-S_1 and leaves almost the same amount of MNP_{30}-S_2 probes in the supernatant.

After confirming the feasibility of the CRISPR-MRS biosensor for detection of *Salmonella* in pure culture, its analytical performance in food samples was also investigated. Chicken breast is an essential food in our daily life but always contaminated by *Salmonella*. Therefore, *S*. Typhimurium spiked in chicken breast extracts were detected. The unspiked sample which was demonstrated free of *Salmonella* by a standard culture method was used as the negative control. As shown in Fig. 4C, the limit of detection (LOD) for *S*. Typhimurium in spiked chicken meat extract was approximately 1.8×10^3 CFU mL^{-1}, demonstrating the high potential of the developed CRISPR-MRS biosensor for real food sample detection. The LOD in chicken meat extracts is one order of magnitude higher than that in buffer, which may be caused by the food matrix. The insoluble solids, proteins, carbohydrates and other known/unknown components in chicken meat may have adverse effects on DNA extraction and the following detection, which lead to a higher LOD.

Finally, the selectivity of the proposed CRISPR-MRS biosensor for *Salmonella* was also evaluated. Here, four other common foodborne pathogenic bacteria, i.e., *Staphylococcus aureus*, *Escherichia coli* O157: H7, *Vibrio parahaemolyticus* and *Listeria monocytogenes* were chosen as the non-targets. As displayed in Fig. 4D, the non-targeted bacteria triggered a negligible change on the T_2 signal. Compared with the negative control, the changes of the T_2 value for *S. aureus*, *E. coli* O157: H7, *V. parahaemolyticus* and *L. monocytogenes* were within 5%, whereas *S*. Typhimurium showed a significant change of the T_2 value which reached more than 60%. The high selectivity of the biosensor was attributed to the double recognition by PCR primers and crRNA. First, only those *Salmonella* germs containing *invA* genes can be recognized by the PCR primers and successfully amplified. Second, the CRISPR-Cas12a system was activated only when the target amplicons existed and were recognized by the Cas12a/crRNA complexes, which further improve the specificity of the CRISPR-MRS biosensor.

4. Conclusion

In this work, the CRISPR-Cas12a system was exploited for the first time to precisely control the binding of the two sizes of MNPs to develop a novel biosensing platform termed CRISPR-MRS for *Salmonella* detection. It avoided the insufficient crosslinking or non-specific binding of MNPs with targets in conventional MRS biosensors, offering improved sensitivity and stability. The CRISPR-MRS biosensor not only enabled sensitive detection of *Salmonella* through MRS measurement, but also provided the ability to intuitively assess the presence of the target via visual observation of the dispersion state of MNPs. Under the optimized conditions, the CRISPR-MRS biosensor showed a LOD of 1.3×10^2 CFU mL^{-1} for *Salmonella*, which was better than most of MRS biosensor analogues. Benefitting from the extremely high specificity of the CRISPR-Cas12a system, it also showed satisfactory selectivity towards *Salmonella* over four non-targeted foodborne pathogenic bacteria. More importantly, the CRISPR-MRS biosensor has the potential to detect other microorganisms by simply designing suitable crRNAs. This CRISPR-MRS biosensor could also be applicable for other Cas proteins with collateral cleavage activity, such as Cas13 and Cas14, for the detection of target RNA/DNA sequences, further expanding its detection potential.

Although presenting improved performance, this CRISPR-MRS also

has its limitations. PCR amplification is still needed in this method for better detection sensitivity, which may complicate the detection process. In future work, we will take several routes to simplify the operation. First, we will adopt the isothermal amplification, such as recombinase polymerase amplification (RPA) to the CRISPR-MRS biosensor to realize "one-pot" reaction to simplify the detection procedure. Second, we also plan to integrate novel signal enhancement strategies (*e.g.*, droplet microfluidics) into this method to develop an amplification-free CRISPR-MRS biosensors that overcome the inherent weakness of amplification-based approaches. Considering its sensitivity, specificity and flexibility, we anticipate the developed CRISPR-MRS biosensor can be widely adopted for the detection of various microbial contaminations in the food supply chain.

CRediT authorship contribution statement

Yafang Shen: Methodology, Investigation, Formal analysis, Writing – original draft. **Fei Jia:** Conceptualization, Investigation, Formal analysis, Funding acquisition, Writing – review & editing. **Yawen He:** Methodology, Formal analysis. **Yingchun Fu** and **Weihuan Fang:** Methodology, Writing – review & editing. **Jianping Wang:** Methodology, Funding acquisition, Writing – review & editing. **Yanbin Li:** Conceptualization, Project administration, Funding acquisition, Writing – review & editing.

Declaration of competing interest

The authors declare that they have no known competing financial interests or personal relationships that could have appeared to influence the work reported in this paper.

Acknowledgments

This study was funded in part by the Walmart Foundation (project # 0402-70013-21-0000) and the National Natural Science Foundation of China (32102058), and supported by the Walmart Food Safety Collaboration Center. The authors thank Dr. Yongwei Wang for his help in the T_2 measurements.

Appendix A. Supplementary data

Supplementary data to this article can be found online at https://doi.org/10.1016/j.bios.2022.114437.

References

Bao, M., Jensen, E., Chang, Y., Korensky, G., Du, K., 2020. Magnetic bead-quantum dot (MB-Qdot) clustered regularly interspaced short palindromic repeat assay for simple viral DNA detection. ACS Appl. Mater. Interfaces 12 (39), 43435–43443.

Bruch, R., Baaske, J., Chatelle, C., Meirich, M., Madlener, S., Weber, W., Dincer, C., Urban, G.A., 2019. CRISPR/Cas13a-powered electrochemical microfluidic biosensor for nucleic acid amplification-free miRNA diagnostics. Adv. Mater. 31 (51), e1905311.

Cao, Y., Wu, J., Pang, B., Zhang, H., Chris Le, X., 2021. CRISPR/Cas12a-mediated gold nanoparticle aggregation for colorimetric detection of SARS-CoV-2. Chem. Commun. 57 (56), 6871–6874.

Centers for Disease Control and Prevention CDC, 2022. Salmonella. Retrieved from. https://www.cdc.gov/salmonella/.

Chen, J.S., Ma, E., Harrington Lucas, B., Da Costa, M., Tian, X., Palefsky Joel, M., Doudna Jennifer, A., 2018. CRISPR-Cas12a target binding unleashes indiscriminate single-stranded DNase activity. Science 360 (6387), 436–439.

Chen, Y., Xianyu, Y., Wang, Y., Zhang, X., Cha, R., Sun, J., Jiang, X., 2015. One-step detection of pathogens and viruses: combining magnetic relaxation switching and magnetic separation. ACS Nano 9 (3), 3184–3191.

Choi, J.-H., Shin, M., Yang, L., Conley, B., Yoon, J., Lee, S.-N., Lee, K.-B., Choi, J.-W., 2021. Clustered regularly interspaced short palindromic repeats-mediated amplification-free detection of viral DNAs using surface-enhanced Raman spectroscopy-active nanoarray. ACS Nano 15 (8), 13475–13485.

Chun, H.J., Kim, S., Han, Y.D., Kim, K.R., Kim, J.-H., Yoon, H., Yoon, H.C., 2018. *Salmonella* Typhimurium sensing strategy based on the loop-mediated isothermal amplification using retroreflective janus particle as a nonspectroscopic signaling probe. ACS Sens. 3 (11), 2261–2268.

Dai, Y., Somoza, R.A., Wang, L., Welter, J.F., Li, Y., Caplan, A.I., Liu, C.C., 2019. Exploring the trans-cleavage activity of CRISPR-Cas12a (cpf1) for the development of a universal electrochemical biosensor. Angew. Chem. Int. Ed. 58 (48), 17399–17405.

Dai, Y., Wu, Y., Liu, G., Gooding, J.J., 2020. CRISPR mediated biosensing toward understanding cellular biology and point-of-care diagnosis. Angew. Chem. Int. Ed. 59 (47), 20754–20766.

Dong, Y., Chen, R., Wu, L., Wang, X., Jiang, F., Fan, Z., Huang, C., Chen, Y., 2022. Magnetic relaxation switching biosensor via polydopamine nanoparticle mediated click chemistry for detection of chlorpyrifos. Biosens. Bioelectron. 207, 114127.

Dong, Y., Wen, C.Y., She, Y., Zhang, Y., Chen, Y., Zeng, J., 2021. Magnetic relaxation switching immunoassay based on hydrogen peroxide-mediated assembly of Ag@Au-Fe_3O_4 nanoprobe for detection of Aflatoxin B1. Small 17 (51), e2104596.

Fu, X., Shi, Y., Peng, F., Zhou, M., Yin, Y., Tan, Y., Chen, M., Yin, X., Ke, G., Zhang, X.-B., 2021. Exploring the trans-cleavage activity of CRISPR/Cas12a on gold nanoparticles for stable and sensitive biosensing. Anal. Chem. 93 (11), 4967–4974.

Gong, S., Li, J., Pan, W., Li, N., Tang, B., 2021. Duplex-specific nuclease-assisted CRISPR-Cas12a strategy for microRNA detection using a personal glucose meter. Anal. Chem. 93 (30), 10719–10726.

Gupta, R., Raza, N., Bhardwaj, S.K., Vikrant, K., Kim, K.-H., Bhardwaj, N., 2021. Advances in nanomaterial-based electrochemical biosensors for the detection of microbial toxins, pathogenic bacteria in food matrices. J. Hazard Mater. 401, 123379.

Hong, F., Huang, C., Wu, L., Wang, M., Chen, Y., She, Y., 2021. Highly sensitive magnetic relaxation sensing method for aflatoxin B1 detection based on Au NP-assisted triple self-assembly cascade signal amplification. Biosens. Bioelectron. 192, 113489.

Huang, L., Liu, S., Ren, S., Zhang, M., Wang, T., Wang, X., Gao, Z., 2021. Magnetic relaxation switch biosensors based on self-assembly of polystyrene microspheres and magnetic nanoparticles for detection of bisphenol A. ACS Appl. Nano Mater. 4 (6), 5963–5971.

Hussain, S.H., Huertas, C.S., Mitchell, A., Deman, A.-L., Laurenceau, E., 2022. Biosensors for circulating tumor cells (CTCs)-biomarker detection in lung and prostate cancer: trends and prospects. Biosens. Bioelectron. 197, 113770.

Jandas, P.J., Prabakaran, K., Luo, J., G, M., H, D., 2021. Effective utilization of quartz crystal microbalance as a tool for biosensing applications. Sens. Actuators, A 331, 113020.

Jia, F., Bai, X., Zhang, X., Fu, Y., Li, Y., Li, X., Kokini, J.L., 2021. A low-field magnetic resonance imaging aptasensor for the rapid and visual sensing of *Pseudomonas aeruginosa* in food, juice, and water. Anal. Chem. 93 (24), 8631–8637.

Josephson, L., Perez, J.M., Weissleder, R., 2001. Magnetic nanosensors for the detection of oligonucleotide sequences. Angew. Chem. Int. Ed. 113 (17), 3304–3306.

Kachwala, M.J., Smith, C.W., Nandu, N., Yigit, M.V., 2021. Reprogrammable gel electrophoresis detection assay using CRISPR-Cas12a and hybridization chain reaction. Anal. Chem. 93 (4), 1934–1938.

Kaittanis, C., Naser, S.A., Perez, J.M., 2007. One-step, nanoparticle-mediated bacterial detection with magnetic relaxation. Nano Lett. 7 (2), 380–383.

Kant, K., Shahbazi, M.-A., Dave, V.P., Ngo, T.A., Chidambara, V.A., Than, L.Q., Bang, D. D., Wolff, A., 2018. Microfluidic devices for sample preparation and rapid detection of foodborne pathogens. Biotechnol. Adv. 36 (4), 1003–1024.

Khansili, N., Rattu, G., Krishna, P.M., 2018. Label-free optical biosensors for food and biological sensor applications. Sens. Actuators, B 265, 35–49.

Li, X., Zheng, T., Xie, Y.-N., Li, F., Jiang, X., Hou, X., Wu, P., 2021. Recombinase polymerase amplification coupled with a photosensitization colorimetric assay for fast *Salmonella* spp. testing. Anal. Chem. 93 (16), 6559–6566.

Nouri, R., Jiang, Y., Tang, Z., Lian, X.L., Guan, W., 2021. Detection of SARS-CoV-2 with solid-state CRISPR-Cas12a-assisted nanopores. Nano Lett. 21 (19), 8393–8400.

Phan, Q.A., Truong, L.B., Medina-Cruz, D., Dincer, C., Mostafavi, E., 2022. CRISPR/Cas-powered nanobiosensors for diagnostics. Biosens. Bioelectron. 197, 113732.

Qi, X., Wang, Z., Lu, R., Liu, J., Li, Y., Chen, Y., 2021. One-step and DNA amplification-free detection of *Listeria monocytogenes* in ham samples: combining magnetic relaxation switching and DNA hybridization reaction. Food Chem. 338, 127837.

Shen, Y., Xu, L., Li, Y., 2021. Biosensors for rapid detection of *Salmonella* in food: a review. Compr. Rev. Food Sci. Food Saf. 20 (1), 149–197.

Sheng, Y., Zhang, T., Zhang, S., Johnston, M., Zheng, X., Shan, Y., Liu, T., Huang, Z., Qian, F., Xie, Z., Ai, Y., Zhong, H., Kuang, T., Dincer, C., Urban, G.A., Hu, J., 2021. A CRISPR/Cas13a-powered catalytic electrochemical biosensor for successive and highly sensitive RNA diagnostics. Biosens. Bioelectron. 178, 113027.

Srisa-Art, M., Boehle, K.E., Geiss, B.J., Henry, C.S., 2018. Highly sensitive detection of *Salmonella* Typhimurium using a colorimetric paper-based analytical device coupled with immunomagnetic separation. Anal. Chem. 90 (1), 1035–1043.

Srisa-Art, M., Dyson, E.C., deMello, A.J., Edel, J.B., 2008. Monitoring of real-time streptavidin-biotin binding kinetics using droplet microfluidics. Anal. Chem. 80 (18), 7063–7067.

Tsourkas, A., Hofstetter, O., Hofstetter, H., Weissleder, R., Josephson, L., 2004. Magnetic relaxation switch immunosensors detect enantiomeric impurities. Angew. Chem. Int. Ed. 43 (18), 2395–2399.

Wang, L., Lin, J., 2020. Recent advances on magnetic nanobead based biosensors: from separation to detection. TrAC Trends Anal. Chem. (Reference Ed.) 128, 115915.

Wang, L., Xue, L., Guo, R., Zheng, L., Wang, S., Yao, L., Huo, X., Liu, N., Liao, M., Li, Y., Lin, J., 2020. Combining impedance biosensor with immunomagnetic separation for rapid screening of *Salmonella* in poultry supply chains. Poultry Sci. 99 (3), 1606–1614.

Wang, S., Zheng, L., Cai, G., Liu, N., Liao, M., Li, Y., Zhang, X., Lin, J., 2019. A microfluidic biosensor for online and sensitive detection of *Salmonella* Typhimurium using fluorescence labeling and smartphone video processing. Biosens. Bioelectron. 140, 111333.

Wang, X., Zhou, S., Chu, C., Yang, M., Huo, D., Hou, C., 2021. Target-induced transcription amplification to trigger the trans-cleavage activity of CRISPR/Cas13a (TITAC-Cas) for detection of alkaline phosphatase. Biosens. Bioelectron. 185, 113281.

Xianyu, Y., Lin, Y., Chen, Q., Belessiotis-Richards, A., Stevens, M.M., Thomas, M.R., 2021. Iodide-mediated rapid and sensitive surface etching of gold nanostars for biosensing. Angew. Chem. Int. Ed. 60 (18), 9891–9896.

Xu, J., Zhang, X., Yan, C., Qin, P., Yao, L., Wang, Q., Chen, W., 2022. Trigging isothermal circular amplification-based tuning of rigorous fluorescence quenching into complete restoration on a multivalent aptamer probe enables ultrasensitive detection of *Salmonella*. Anal. Chem. 94 (2), 1357–1364.

Xue, L., Guo, R., Huang, F., Qi, W., Liu, Y., Cai, G., Lin, J., 2021. An impedance biosensor based on magnetic nanobead net and MnO_2 nanoflowers for rapid and sensitive detection of foodborne bacteria. Biosens. Bioelectron. 173, 112800.

Yue, H., Huang, M., Tian, T., Xiong, E., Zhou, X., 2021. Advances in clustered, regularly interspaced short palindromic repeats (CRISPR)-based diagnostic assays assisted by micro/nanotechnologies. ACS Nano 15 (5), 7848–7859.